Shape preferred orientation of dolostone bodies of a Triassic broken formation at the western External Betics

Orientación preferente de forma de cuerpos de dolomías de una broken formation *triásica en las Béticas Externas occidentales*

Manuel Díaz Azpiroz, Rosa Asencio Almansa, Juan Ramón Senín Andrades y Alejandro Jiménez Bonilla

Dpto. Sistemas Físicos, Químicos y Naturales. Universidad Pablo de Olavide. Crtra. Utrera km 1, 41013 Sevilla (mdiaazp@upo.es, rosalmansa@gmail.com, jrsenand@alu.upo.es, alex_jb16@hotmail.com).

ABSTRACT

Detailed structural analyses of block-in-matrix formations are key to understand the tectonic processes involved in the external zones of many convergent orogens. One of these formations, with a highly controversial origin and evolution, marks the boundary between the fold-and-thrust belt and the foreland basin of the Betics. We analyzed dolostone bodies from this block-in-matrix formation in the western External Betics (Badolatosa, Sevilla), affected by the Algodonales-Badolatosa shear zone, to obtain a partial SPO (θ angle between long axes and the shear zone boundary). Our results define a main 500-1200 m-wide band strongly controlled by deformation at the WNW-NNW boundary of this shear zone. Minor, heterogeneously distributed bands with a moderate SPO are tentatively interpreted as Riedel shears related to dextral transpression.

Key-words: *block-in-matrix, circular statistics, External Betics, shape preferred orientation, shear zones .*

RESUMEN

El análisis estructural detallado de formaciones con fábricas de tipo block-in-matrix *es clave para entender los procesos tectónicos que ocurren en las zonas externas de numerosos orógenos convergentes. Una de estas formaciones, con origen y evolución muy controvertidos, marca el límite entre el cinturón de pliegues y cabalgamientos y la cuenca de antepaís de las Béticas. Hemos analizado los cuerpos de dolomías de esta formación de tipo* block-in-matrix *de las Béticas occidentales (Badolatosa, Sevilla), afectada por la zona de cizalla de Algodonales-Badolatosa, para obtener una SPO parcial (ángulo* θ *entre los ejes largos y el límite de la zona de cizalla). Nuestros resultados muestran una banda de 500-1200 m de ancho fuertemente controlada por la deformación en el límite ONO-NNO de dicha zona de cizalla. Bandas con una SPO moderada, distribuidas heterogéneamente, podrían interpretarse como cizallas Riedel relacionadas con una transpresión dextra.*

Palabras clave: block-in-matrix, *estadística de datos circulares, Béticas Externas, orientación preferente de forma, zonas de cizalla.*

Geogaceta, 67 (2020), 11-14
ISSN (versión impresa): 0213-683X
ISSN (Internet): 2173-6545

Fecha de recepción: 28/06/2019
Fecha de revisión: 17/10/2019
Fecha de aceptación: 22/11/2019

Introduction

Mélanges and broken formations (Festa *et al*., 2010, 2012) are conspicuous in convergent settings and yet, their tectonic interpretation remains incipient, mainly due to the high complexity of their characteristic block-in-matrix fabric (*e.g.*, Kusky and Bradley, 1999; Alonso *et al*., 2006, 2015). Detailed structural analyses of these apparent chaotic formations have normally revealed a structured fabric, and contributed to understand the tectonic processes involved in these units (*e.g.*, Kusky and Bradley, 1999; Alonso *et al*., 2006; Escuder-Viruete and Baumgartner, 2014; Fuentes *et al*., 2019).

In the Betics, the boundary between the fold-and-thrust belt proper and the foreland Guadalquivir basin is marked by a discontinuous, up to 30 km-wide band where mainly dolostones, versicolor marls and gypsum crop out. The detailed structure of this band is not totally understood and thus its evolution is still highly controversial. It has been traditionally described

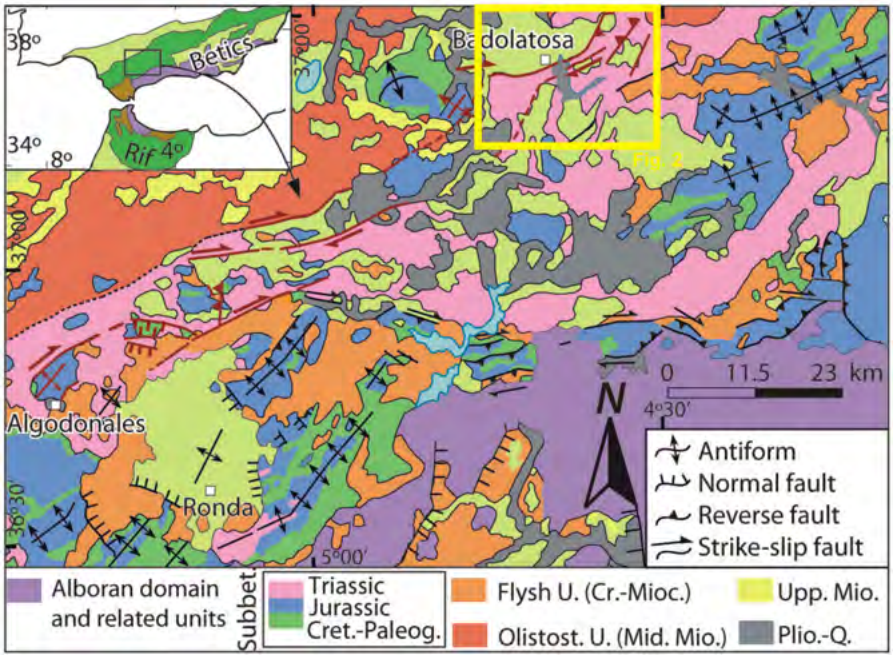

Fig. 1.- Geological map of the western External Betics with the location of the Algodonales-Badolatosa shear zone (García *et al*., 2016) and figure 2.
Fig. 1.- Mapa geológico de las Béticas Externas occidentales. Se localizan la zona de cizalla de Algodonales-Badolatosa (García et al.*, 2016) y la figura 2.*

Copyright© 2020 Sociedad Geológica de España / www.geogaceta.com

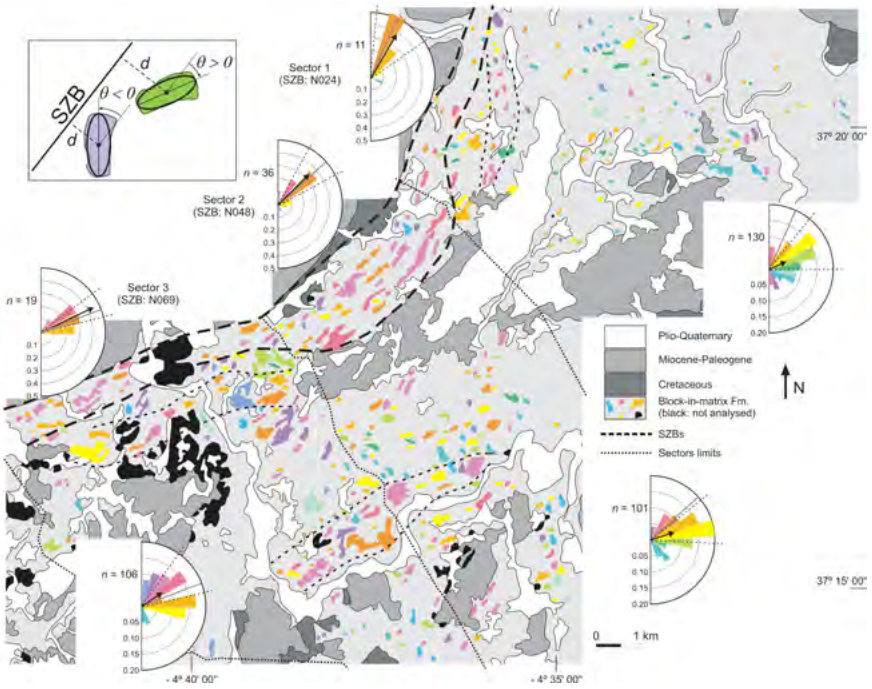

Fig. 2.- SPO of dolostone bodies on a simplified geological map of the study area (modified after Roldán *et al*., 2019). The approximate location of the W-NNW boundary of the ABSZ (SZB), the most intensively deformed band, possible minor deformation bands (see main text) and the three sectors defined based on varying strike are marked. Colors indicate 15º intervals of angle Θ respecting the SZB strike in each sector (see rose diagrams for color code). Information in rose diagrams: relative frequency of each interval (note that contours are different inside and outside the deformed band); mean angle (black vector, whose length is proportional to the mean resultant length) and 95% confidence interval around it (dashed lines); and the average azimuth of the SZB in each sector (grey line); n: number of measurements. The inset illustrates schematically the main parameters measured in this SPO (see the main text for explanation).
Fig. 2.- SPO de cuerpos de dolomías sobre un mapa geológico simplificado del área de estudio (modificado de Roldán et al.*, 2019). Se muestran la localización aproximada del límite O-NNO de la ABSZ (SZB), la banda con deformación más intensa, otras bandas deformadas posibles (véase el texto principal) y los tres sectores definidos en función de la dirección de SZB. Los colores corresponden a intervalos de 15º en el ángulo Θ respecto a la dirección de SZB en cada sector (véanse los diagramas de rosa para el código de color). Información en los diagramas de rosa: frecuencia relativa de cada intervalo (nótese que los contornos son diferentes dentro y fuera de la banda deformada); ángulo medio (vector negro, cuya longitud es proporcional al vector medio resultante) e intervalo de confianza con nivel de significación del 95% (línea a trazos); y la dirección promedio de SZB en cada sector (línea gris); n: número de medidas. El recuadro ilustra de forma esquemática los principales parámetros medidos en esta SPO (véase el texto principal).*

as chaotic and consequently interpreted as either an olistostromic unit (*e.g.*, Roldán-García *et al*., 2012; Rodríguez-Fernández *et al*., 2013, and references therein) or a lateral diapir (Berástegui *et al*., 1998). However, depending on the observed site, a somewhat well defined Triassic stratigraphic sequence (*e.g.*, Pérez-López, 1991), an imbricate structure (Swere, 2017) or a block-in-matrix fabric (*e.g.*, Roldan *et al.*, 2019) are apparent. These observations suggest that this band would correspond to the Subbetic Triassic, partially affected by recent deformation likely related to the emplacement of the Betic fold-and-thrust belt.

In this paper, we present a shape preferred orientation (SPO) analysis of dolostones bodies cropping out near Badolatosa (Sevilla), in the western Betics, to contribute with further structural information to the knowledge of this cryptic band.

Geological setting

The analyzed band (Fig. 1) extends from Algodonales (Cádiz) to Jauja (Córdoba). In the study area, this band presents cm- to hm- bodies of mainly dolostones, likely belonging to distinct Triassic units (Cehegín, Zamoranos and K5 Fms., Pérez-López, 1991); with minor sandstones, lutites, clays and gypsum; embedded in a clay-rich (locally gypsum-rich) matrix, mostly defining a block-in-matrix fabric (Fig. 2). It lacks significant exotic blocks, thus it could be interpreted as a Triassic broken formation (in the sense of Festa *et al*., 2012), likely disrupted by heterogeneous deformation broadly concentrated in a dextral transpressional shear zone, the so-called Algodonales-Badolatosa shear zone (ABSZ, Jiménez-Bonilla *et al*., 2015; García *et al*., 2016). The ABSZ is *ca*. 10 km wide; it strikes ENE-WSW along most of its 90 km of length, although it acquires a more NNE-SSW at its easternmost segment, near the village of Badolatosa (Fig. 1). Outcrops of a clastic sequence with few carbonatic and gypsiferous beds (assigned to the Keuper facies of the Southiberian Triassic, Pérez-López, 1991) are also present.

We focused our analysis in the easternmost segment of the ABSZ, near the villages of Badolatosa (Sevilla) and Jauja (Córdoba). The Triassic broken formation cropping out in the study area bounds to the N with Serravalian-Tortonian marls and minor sandstones. This tectonic limit (García *et al*., 2016) strikes ENE in the western part and varies to NE and NNE toward the east (Fig. 2). We define this limit as the NNW to WNW Algodonales-Badolatosa shear zone boundary (SZB hereafter).

SPO of dolostone bodies

Method

We accomplished a statistical analysis of 2D sections of dolostone bodies on the subhorizontal topographic surface (dolostone bodies hereafter). We are aware this is only a partial analysis that does not take into account that both the shape of the analyzed bodies and the deformation are 3D. This is a common situation in SPO analyses, which it does not affect significantly the fundamental results as long as the Vorticity Normal Section is close to horizontality, likely the case of the ABSZ, a simple shearing, strike-slip dominated shear zone.

The SPO was analyzed separately in three different sectors defined according to the trend of the SZB of the ABSZ. As such, from the NNE, the SZB strikes 024º in sector 1, 048º in sector 2 and 069º in sector 3 (Fig. 2).

Dolostone bodies within the ABSZ were manually selected from the GEODE map (Roldán *et al*., 2019), excluding those that are partially covered by post-Miocene deposits, are anomalously large and/or extremely irregular in shape. Few mapped outcrops of Cretaceous rocks (Roldán *et al*., 2019) are tentatively interpreted as part of an imbricate structure (Sweere, 2017) and thus were not considered. Selected bodies were analyzed via software SPO2003 (Launeau and Robin, 1996), which uses the inertia tensor to estimate the best-fitting ellipse to each dolostone body (Fig. 2, inset). Results for each ellipse include, among others, the distance of the center to the SZB trace in each sector (x), the aspect ratio (R),

the radius of the circle with equivalent area and the angle θ between the long axis (*a*) and the SZB trace. Positive and negative values of θ correspond to angles measured, respectively, clockwise and anticlockwise with respect to the SZB trace (Fig. 2, inset).

We focus this study on the preferred orientation (angle θ) of dolostone bodies with R > 1.5 (to exclude mostly rounded bodies). Firstly, we analyze how this angle varies with the distance to the SZB (Fig. 3). According to the obtained results (see below), we carried out circular statistics of angle θ from three samples (one for each sector) located close to the SZB (500 to 1200 m depending on the sector), and from sampling subsectors with regular widths and progressively farther from the SZB. Computed statistics for each sample include the mean angle ($\bar{\theta}$), the mean resultant length ($\bar{R}$) and the circular variance (S_0^2). We also applied the Rayleigh's test and, for samples with not uniform distribution, we obtained the concentration parameter (*k*) and calculated the standard error (S_e) and a 95% confidence interval around the mean angle (see Mardia, 1972 and Davis, 2003 for theoretical details on statistics of circular data). Again, statistics from each sample are represented against their distance to the SZB (Fig. 4).

Results

Our results permit to define a band limited to the WNW to NNW (depending on the sector) by the SZB, where most dolostones bodies are strongly aligned with the SZB, irrespective of the sector. The width of this band ranges from around 500-600 m (in sectors 1 and 3) to 1200 m (in sector 2). This is evident in map view (Fig. 2), with predominance of orange and red bodies. Also, when angle θ is represented against distance (Fig. 3), there are very few bodies with θ > 30º in this band (particularly in sectors 1 and 3), contrary to what it is the rule out of it. Moreover, assuming the population of bodies presents a Von Mises distribution (*i.e.*, it is either uniform or unimodal), the Rayleigh's test (Mardia, 1972) indicates these data come from a population with a significant preferred orientation. Samples from this band show low dispersion, as evidenced by circular variance and standard error values (Fig. 4A, B). Indeed, there is a general tendency (with some exceptions) of the standard error to progressively diminish toward the SZB (Fig. 4B). In the same sense, the mean angle is close to the strike of the SZB for each sector and the small 95% confidence interval clearly includes such direction (Fig. 4C).

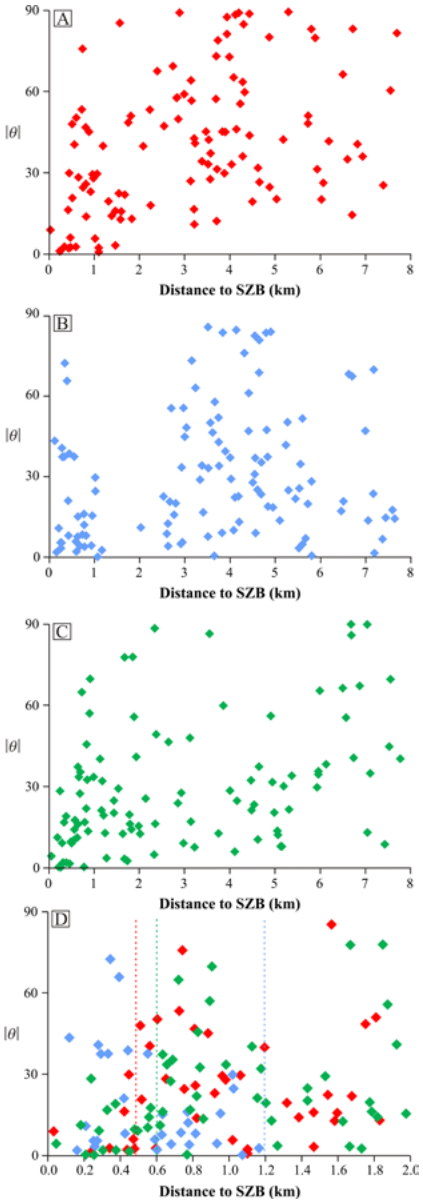

Fig. 3.- A-C) Variation of angle *Θ* with distance to the SZB in sectors 1 (A), 2 (B) and 3 (C). D) Detail in the first 2 km from the SZB for the three sectors (1: red, 2: blue, 3: green). Dashed lines mark the approximate location of the ESE-SSE boundary of the most intensively deformed band.

Fig. 3.- A-C) Variación del ángulo Θ con la distancia a SZB en los sectores 1 (A), 2 (B) y 3 (C). D) Detalle de los primeros 2 km desde SZB para los tres sectores (1: rojo, 2: azul, 3: verde). Las líneas a trazos marcan la localización aproximada del límite ESE-SSE de la banda de deformación más intensa.

Outside this 500-1200 m band limited by the SZB, the dolostone bodies show a more uniform distribution in general, although a preferred orientation cannot be statistically ruled out (Fig. 2). In any case, certain areas do present a significant preferred orientation, together with low variance and standard error values. See, for example, values at 1.2 km in sectors 1 and 3 or at 5.5 km in sector 2 (Fig. 4A, B). However, the mean orientation of two of these samples (sectors 2 and 3) is located at around 20º clockwise away from the SZB strike, which is not included within the 95% confidence interval (Fig. 4C). These samples could tentatively be assigned to minor deformation bands depicted in map view (Fig. 2). Outside these three, the rest of the samples define either uniform distributions or highly disperse data, thus suggesting the absence of a preferred orientation of dolostone bodies.

Discussion and conclusions

The SPO analysis of dolostone bodies within the eastern ABSZ defines a main 500-1200 band, strongly controlled by deformation at the WNW-NNW boundary of this shear zone. Minor bands with a moderate SPO are heterogeneously distributed within the analyzed Triassic outcrops at the study area. The mean angle defined by dolostone bodies in two of these bands is *ca.* 20º clockwise from the SZB, suggesting they could represent Riedel shears compatible with a dextral transpression. This kinematics agrees with previous detailed structural data (discrete fault planes in clay-rich matrix, foliations in gypsum breccias, imbricated structures) from sector 3 (García *et al.*, 2016; Sweere, 2017) and from the westernmost segment of the ABSZ (Jiménez-Bonilla *et al.*, 2015). These results point to a strike-slip related broken formation of the Festa *et al.* (2012) classification. A main tectonic origin for this Triassic broken formation is also coherent with the interpretation that Pérez-Valera *et al.* (2017) gave to the so-called Guadalquivir Units in the eastern Betics.

Stratal disruption and boudinage seem the most likely processes producing reorientation of dolostone bodies (see also Pérez-Valera *et al.*, 2017). However, given their high rheological contrast respecting the matrix, rigid body rotation (*cf.* Jessup *et al.*, 2007) cannot be disregarded. In any case, detailed analyses of other SPO parameters (grain size, aspect ratio, etc.), of the actual 3D shape of the dolostone bodies via geophysical prospection and of the structural organization (currently in progress) will help to constrain possible sedimentary and/or deformation mechanisms responsible for the origin and evolution of the studied block-in-matrix formation.

Acknowledgements

Financial support from projects CGL2017-89051-P (Plan Propio de Investi-

gación de la Universidad Pablo de Olavide) and PGC2018-100914-B-100 (Ministerio de Ciencia, Innovación y Universidades). Reviews by J.L. Alonso y F. Pérez-Valera greatly improved the manuscript.

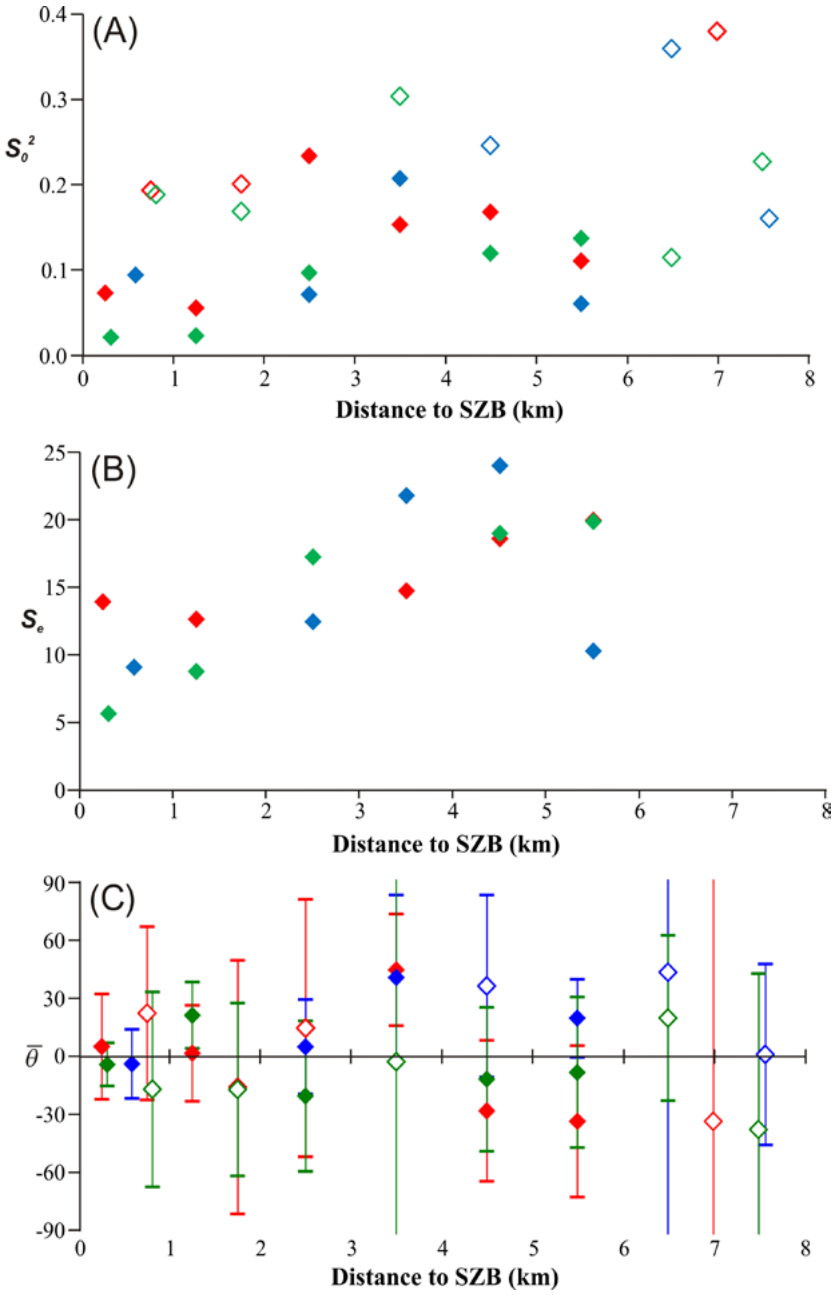

Fig. 4.- Variation with distance to the SZB of circular statistics from different samples defined within each sector. The closest sample to the SZB was defined in base of data from figures 2 and 3. The rest of samples are uniformly distributed within the rest of the study area. Color code as in figure 3. A) Circular variance (solid and open symbols correspond, respectively, to samples with a preferred orientation and a uniform distribution according to the Rayleigh's test). B) Standard error. C) Mean direction (angle *Θ*, positive and negative values correspond, respectively, to clockwise and anticlockwise orientation respecting the SZB azimuth, see Fig. 2) and 95% confidence interval obtained from the standard error. Samples with uniform distribution in A are not represented in B and C.

Fig. 4.- Variación con la distancia a SZB de estadísticos circulares obtenidos a partir de distintas muestras definidas en cada sector. La muestra más cercana a SZB se ha definido en función de los datos de las figuras 2 y 3. El resto de muestras se distribuyen uniformemente por el resto de la zona estudiada. Código de colores como en la figura 3. A) Varianza circular (símbolos sólidos y abiertos corresponden, respectivamente, a muestras con orientación preferente y distribución uniforme de acuerdo con el test de Rayleigh). B) Error Estándar. C) Dirección promedio (ángulo Θ, con valores positivos y negativos correspondientes, respectivamente, a orientaciones respecto a SZB en el sentido de las agujas del reloj y el contrario, véase Fig. 2) e intervalo de confianza del 95% obtenido a partir del error estándar. Las muestras con distribución uniforme en A no se representan en B ni en C.

References

Alonso, J.L., Marcos, A. and Suárez, A. (2006). *American Journal of Science* 306, 32-65.

Alonso, J.L., Marcos, A., Villa, E., Suárez, A., Merino-Tomé, O.A. and Fernández, L.P. (2015). *International Geology Review* 57, 563-580.

Berástegui, X., Banks, C.J., Puig, C., Taberner, C., Waltham, D. and Fernàndez, M. (1998). *Geological Society, London, Special Publication* 134, 49-68.

Davis, J.C. (2003). *Statistics and Data Analysis in Geology*. John Wiley & Sons, New York, 638 p.

Escuder-Viruete, J. and Baumgartner, P.O. (2014). *Journal of Structural Geology* 66, 356-381.

Festa, A., Pini, G.A., Dilek, Y. and Codegone, G. (2010). *International Geology Review* 52, 1040-1105.

Festa, A., Dilek, Y., Pini, G.A., Codegone, G. and Ogata, K. (2012). *Tectonophysics* 568, 7-24.

Fuentes, P., Fernández, C., Díaz-Alvarado, J. and Díaz-Azpiroz, M. (2019). *Gondwana Research* 74, 251-270.

García, R., Jiménez Bonilla, A., Díaz-Azpiroz, M., Pérez Valera, F., Balanyá, J.C. and Expósito, I. (2016). *Geo-Temas* 16, 547-550.

Jessup, M.J., Law, R.D. and Frassi, C. (2007). *Journal of Structural Geology* 29, 411-421.

Jiménez-Bonilla, A., Expósito, I., Balanyá, J.C., Barcos, L. and Diaz-Azpiroz, M. (2015). *Geogaceta* 57, 27-30.

Kusky, T.M. and Bradley, D.C. (1999). *Journal of Structural Geology* 21, 1773-1796.

Launeau, P. and Robin, P-Y.F. (1996). *Tectonophysics* 267, 91-119.

Mardia, K.V. (1972). *Statistics of Directional Data*. Academic Press, London, 357 p.

Pérez-López, A. (1991). *El Trías de facies germánica del sector central de la Cordillera Bética*. PhD thesis, University of Granada.

Pérez-Valera, F., Sánchez-Gómez, M., Pérez-López, A. and Pérez-Valera, L.A. (2017). *Tectonics* 36, doi:10.1002/2016TC004414.

Rodríguez-Fernández, J., Roldán, F.J., Azañón, J.M. and García-Cortés, A. (2013). *Boletín Geológico y Minero* 124, 477-504.

Roldán-García, F.J., Rodríguez-Fernández, J. and Azañón, J.M. (2012). *Geogaceta* 52, 103-106.

Roldán, F.J., Rodríguez-Fernández, J., Villalobos, M., Lastra, J., Díaz-Pinto, G., Pérez-Rodríguez, A.B. (2019). *GEODE Mapa Geológico Digital continuo de España E. 1:50000. Zonas: Subbético, Cuenca del Guadalquivir y Campo de Gibraltar.* [en línea]. [Consulta 28/06/2019]. Disponible en: info.igme.es/cartografiadigital/geologica/geodezona.aspx?Id=Z2600.

Sweere, N. (2017). *Análisis estructural y del relieve de las formaciones del Subbético en la cuenca de las lagunas Amarga y Dulce (Jauja, Córdoba)*. Unpublished degree dissertation, U. Pablo de Olavide.